Electronic Supplementary Information (ESI)

Facile synthesis of porous nickel manganite materials and their morphologies effect on electrochemical properties

Huan Pang, Jiawei Deng, Shaomei Wang, Sujuan Li, Jing Chen and Jiangshan Zhang

Experiment

1 Synthesis

For bipyramid structured precursors, firstly, 10 mL 0.1 mol·L^{-1} Ni(OAc)$_2$ solution, 20 mL 0.1 mol·L^{-1} Mn(OAc)$_2$ solution were mixed round at room temperature for half an hour; secondly 40 mL 0.1 mol·L^{-1} $(NH_4)_2C_2O_4$ solution was added, and then we can obtain green precipitation after being mixed round several hours. For fusiform structured precursors, firstly using 5 mL 0.1 mol·L^{-1} Ni(OAc)$_2$ solution, 10 mL 0.1 mol·L^{-1} Mn(OAc)$_2$ solution were mixed with 100 mL H_2O round room temperature for half an hour; secondly 40 mL 0.1 mol·L^{-1} $(NH_4)_2C_2O_4$ solution was added, and then also was mixed round several hours. At last, we can obtain green fusiform-like structured precursors (Fig.2 d, e). The plate structures can be obtained by decreasing amount of Ni(OAc)$_2$ solution, Mn(OAc)$_2$ solution, $(NH_4)_2C_2O_4$ solution to 2.5 mL, 5 mL, 10 mL.

2 Electrode preparation

The working electrodes were prepared as follows. The electrode of $NiMn_2O_4$ materials was prepared according to the following steps. The mixture containing 80 wt.% $NiMn_2O_4$, 15 wt.% acetylene black and 5 wt.% polytetrafluoroethylene(PTFE) was well mixed, and then was pressed onto nickel grid (1.2×10^7 Pa) that serves as a current collector (surface is 1 cm^2). The typical mass load of electrode material is 5 mg.

3 Characterization

The morphology of the as-prepared samples was observed by a Hitachi S-4800 field-emission scanning electron microscope (FE-SEM) at an acceleration voltage of 10.0 kV. The phase analyses of the samples were performed by X-ray diffraction (XRD) on a SHIMADZU, XRD-6000 with Cu K_α radiation (λ = 1.5418 Å). Transmission electron microscopy (TEM) images and HRTEM image were captured on the JEM-2100 instrument microscopy at an acceleration voltage of 200 kV.

The electrochemical measurements were carried out by an electrochemical analyzer system, CHI660D (Chenhua, Shanghai, China) in a three-compartment cell with a platinum plate counter electrode, a Ag/AgCl electrode reference electrode. The electrolyte was a 1 M Na_2SO_4 aqueous solution.

4 Calculation

1. Specific capacitances derived from galvanostatic (GV) tests can be calculated from the equation:

$C = (I \Delta t)/(m \Delta U)$

where C (F/g), I (A), Δt (s), m (g) and ΔU are the specific capacitance, the discharge current, the discharge time, the mass of the active materials in electrode, and the potential window, respectively.

2. $NiMn_2O_4 + Na^+ + e^- === NaNiMn_2O_4$;

$i_0 = RT/nFR_{ct}$ (n=1; F=96485; R=8.314);

$i_0 = A \exp(-E_a/RT)$;

$E_a = -2.303Rk$;

$k_{M1} = -6.298$; $E_{a\text{-}M1} = -2.303 \times 8.314 \times (-6.298) = 120.59$ kJ mol^{-1};

$k_{M2} = -4.637$; $E_{a\text{-}M2} = -2.303 \times 8.314 \times (-4.637) = 88.79$ kJ mol^{-1};

$k_{M3} = -2.677$; $E_{a\text{-}M3} = -2.303 \times 8.314 \times (-2.677) = 51.26$ kJ mol^{-1};

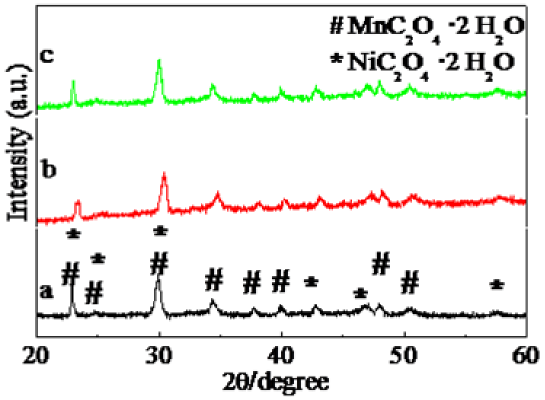

ESI Fig. 1 the powder X-ray diffraction patterns of precursors, (a) bipyramid; (b) fusiform; (c) plate.

Precursors	**Ni wt%**	**Mn wt%**	**C wt%**	**O wt%**
bipyramid	9.1	16.9	10.6	64.4
fusiform	8.1	15.5	10.6	65.8
plate	9.2	17	10.8	63
$NiMn_2O_4$	**Ni wt%**	**Mn wt%**		**O wt%**
bipyramid-M1	24. 1	46. 1		30. 8
fusiform-M2	25. 1	47. 1		27. 8
plate-M3	24. 7	48. 2		27. 1

ESI. Table 1 EDS data of precursors and $NiMn_2O_4$ nanostructures, the value in ESI Table 1 is the average one which was based on 6 times test results.

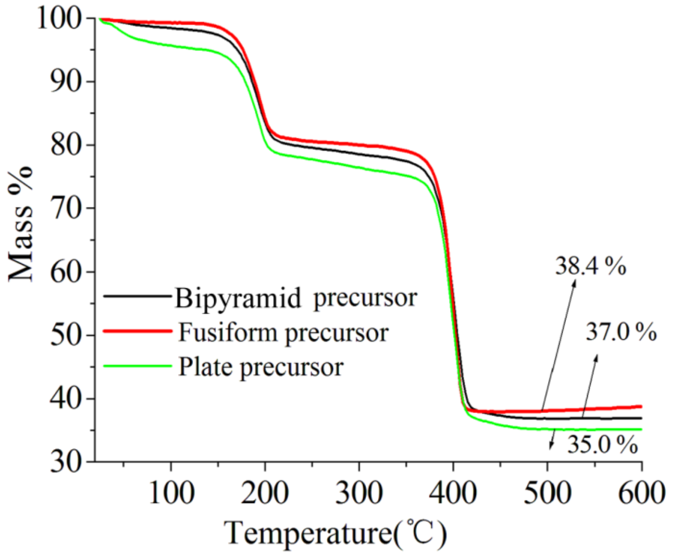

ESI Fig. 2 TG curves of precursors

$NiMn_2(C_2O_4)_3{\cdot}nH_2O$=====$NiMn_2O_4$ + 4CO + $2CO_2$ + nH_2O
464.6+18n 432.6 88 112 18n

432.6/(18n+464.6)=37.0% (38.4% or 35.0%)

n≈14, 12, 16

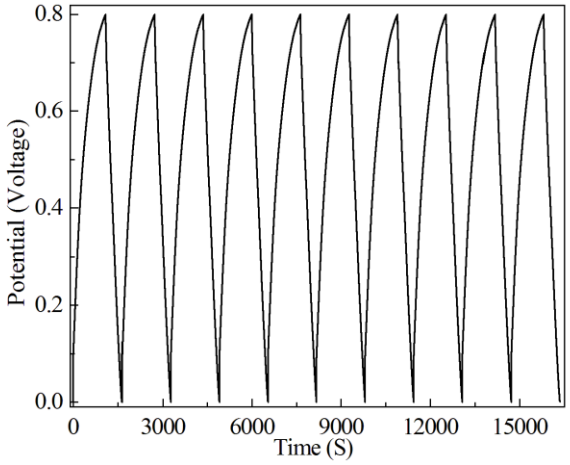

ESI Fig. 3 the first ten cycle charge-discharge curves for porous plate $NiMn_2O_4$ electrode.

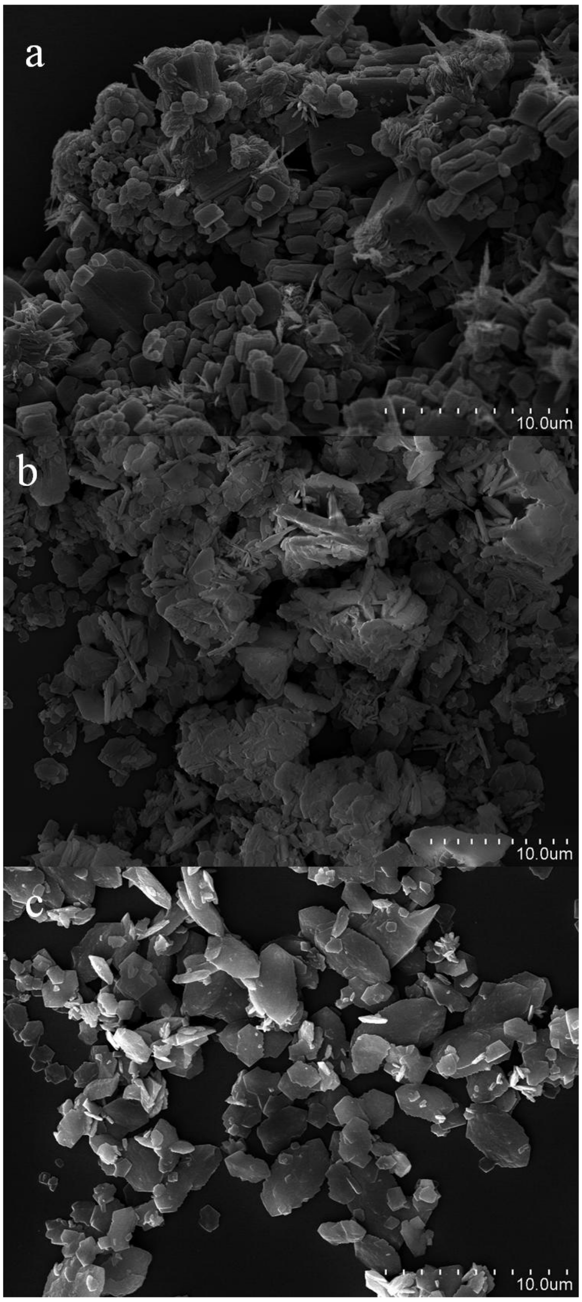

ESI Fig. 4 SEM images of $NiMn_2O_4$ after 1000 charge–discharge cycles, (a) M1, (b)M2, (c)M3.

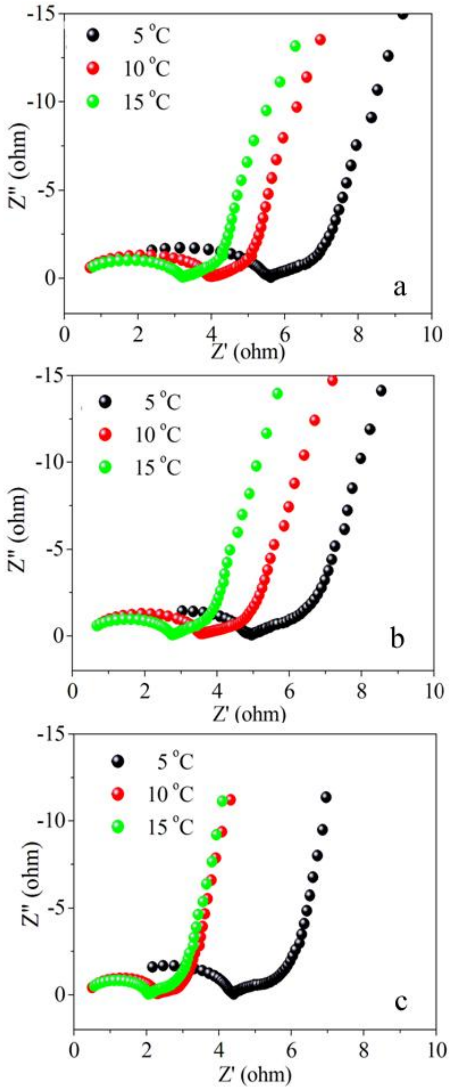

ESI Fig. 5 Electrochemical impedance spectra (EIS) for $NiMn_2O_4$ electrodes under different temperatures in 1.0 M Na_2SO_4 solution at 0.8 V, (a)-M1; (b)-M2; (c)-M3.

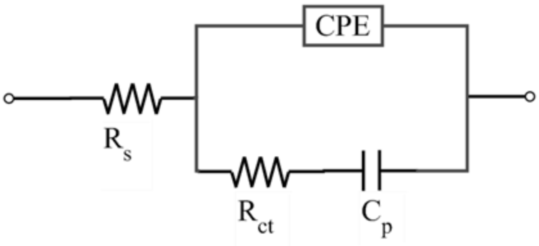

ESI Fig. 6 An equivalent circuitan consisting of a bulk solution resistance R_s, a charge-transfer R_{ct}, a pseudocapacitive element C_p from redox process of $NiMn_2O_4$, and a constant phase element (CPE) to account for the double-layer capacitance.

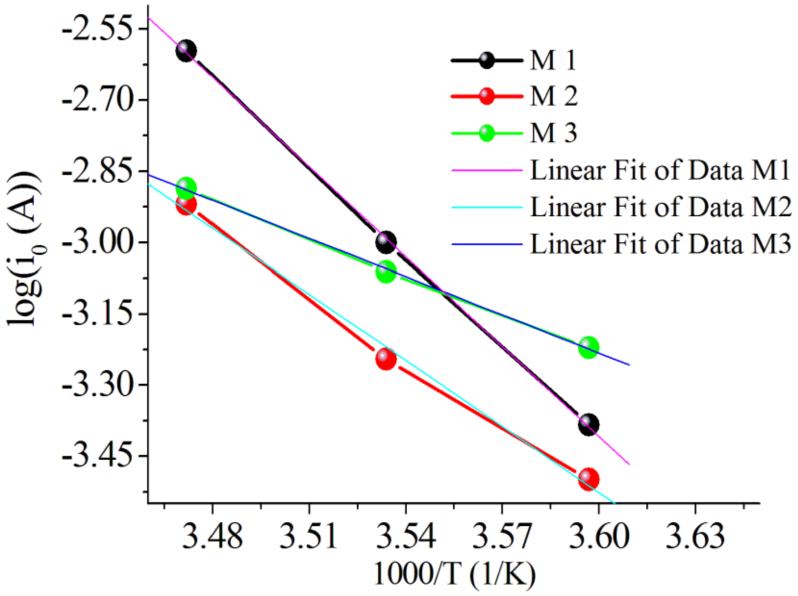

ESI Fig. 7 Arrhenius plots of log i_0 versus 1/ T for the $NiMn_2O_4$ electrodes at 0.8 V.

The charge-transfer resistance R_{ct} was calculated from the data in ESI Fig. 5 (by ZSimpWin soft ware). Then, the exchange currents (i_0) and the apparent activation energies (E_a) for the intercalation of Na^+ can be calculated by and the Arrhenius equation (eq. 1, 2 & 3), respectively.

$i_0 = RT/nFR_{ct}$; (n=1; F=96485; R=8.314) (eq.1);

$i_0 = A\exp(-E_a/RT)$; (eq.2);

$E_a = -2.303Rk$; (k is slope); (eq.3).

Where A is a temperature-independent coefficient, R is the gas constant, T is the absolute temperature, n is the number of transferred electrons, and F is the Faraday constant.

An Arrhenius plot of log i_0 as a function of 1/T is shown in ESI Fig. 7. On the basis of eq. 2 & 3, k is slope of the straight line in ESI Fig. 7, the activation energies (E_a) are calculated to be 120.6, 88.8 and 51.3 kJ mol^{-1}, respectively (Calculation equation can be seen in ESI Experiment Calculation). The lowest activation energy of porous plate $NiMn_2O_4$ electrode indicates the shorter diffusion route for ion intercalation.